J Nanopart Res (2015) 17:234
DOI 10.1007/s11051-015-3043-0

RESEARCH PAPER

Peptide-activated gold nanoparticles for selective visual sensing of virus

Basavaraj Sajjanar · Bhuvna Kakodia · Deepika Bisht · Shikha Saxena · Arvind Kumar Singh · Vinay Joshi · Ashok Kumar Tiwari · Satish Kumar

Received: 24 January 2015 / Accepted: 18 May 2015 / Published online: 28 May 2015

Abstract In this study, we report peptide–gold nanoparticles (AuNP)-based visual sensor for viruses. Citrate-stabilized AuNP (20 ± 1.9 nm) were functionalized with strong sulfur–gold interface using cysteinylated virus-specific peptide. Peptide–Cys–AuNP formed complexes with the viruses which made them to aggregate. The aggregation can be observed with naked eye and also with UV–Vis spectrophotometer as a color change from bright red to purple. The test allows for fast and selective detection of specific viruses. Spectroscopic measurements showed high linear correlation ($R^2 = 0.995$) between the changes in optical density ratio (OD_{610}/OD_{520}) with the different concentrations of virus. The new method was compared with the hemagglutinating (HA) test for Newcastle disease virus (NDV). The results indicated that peptide–Cys–AuNP was more sensitive and can visually detect minimum number of virus particles present in the biological samples. The limit of detection for the NDV was 0.125 HA units of the virus. The method allows for selective detection and quantification of the NDV, and requires no isolation of viral RNA and PCR experiments. This strategy may be utilized for detection of other important human and animal viral pathogens.

Keywords Peptides · AuNP · Surface plasmon · Virus · Colorimetric detection · Nanobiotechnology

B. Sajjanar · B. Kakodia · D. Bisht · S. Saxena · A. K. Singh · A. K. Tiwari · S. Kumar (✉)
Division of Veterinary Biotechnology, Indian Veterinary Research Institute, Bareilly 243122, Uttar Pradesh, India
e-mail: drsatishkumar_ivri@yahoo.co.in

Present Address:
V. Joshi
Department of Animal Biotechnology, Lala Lajpat Rai University of Veterinary & Animal Sciences, Hisar 125004, Haryana, India

Introduction

Viruses are small infectious agents responsible for a large number of diseases both in humans and animals. Many of the emerging and re-emerging viruses such as influenza and ebola have created panic among the public in recent times. The treatment and control of viral diseases call for quick diagnosis. Wide ranges of techniques are available for detection and identification of viruses. Isolation in cell culture, plaque assay, hemagglutination (HA) test, and other biochemical methods including enzyme-linked immuno sorbent assay (ELISA) have been used for the diagnosis of viral diseases (Belák 2007). Nucleic acid-based techniques (PCR/RT-PCR) have become popular (O'Connor and Glynn 2010; Cobo 2012). These methods are sensitive in the detection of pathogens. However, they require sophisticated laboratory, expensive reagents, and higher technical expertise. On site, more user-friendly and cost-effective methods of diagnosis may help in controlling the viral diseases.

In the recent years, nanotechnology, with the application of metallic nanoparticles, has expedited the diagnostic procedures with improved sensitivity and specificity. Size, shape, and interparticle distance govern plasmon resonance of nanoparticles. Hence, by changing the interparticle distance, the plasmon resonance of metallic nanoparticles can be tuned across the visible spectrum into near-infrared (West and Halas 2000; Jin et al. 2001). This makes multicolor assay possible with single source even under white-light illumination without need for filters. Among the known metallic nanoparticles, gold nanoparticles (AuNP) are preferred mostly for designing theranostics, because of facile synthesis and versatile activation with proteins, nucleic acids, carbohydrates, and drugs (Rita and Pedro 2014). Interactions between the target analyte and the activated AuNP results in specific visible plasmon change and has been well adopted for various detection schemes including heavy metals, cells, polynucleotides, and bacteriophages (Darbha et al. 2008; Medley et al. 2008; Joshi et al. 2013; Lesniewski et al. 2014).

Recently, Lee et al. (2013) used sialic acid-activated AuNP for colorimetric detection of the influenza virus. However, sialic acid (SA) is a part of host cell glycoproteins which act as the common binding determinant for many species of viruses (Stehle and Khan 2014). Other than influenza, important human and animal pathogens such as measles, mumps, rhino, corona, parainfluenza, NDV, and peste des petits of ruminants (PPRV) interact with SA (Matrosovich et al. 2013). The method devised using SA–AuNPs may give ambiguous results, for example, NDV affecting the birds with similar clinical signs as that of avian influenza may likely be termed as influenza, leading to false positive result. In such situation, more specific methods of using AuNP conjugates are required. Antibody-conjugated gold nanoparticles are more specific and help in selective detection of viruses without false positive results: for example, antibody-conjugated AuNP used for visual sensing of bacteriophages (Lesniewski et al. 2014). The method involved Cys–AuNP synthesis and antibody conjugation procedures by activation of functional groups with coupling agents.

In the present study, a virus-specific peptide previously identified by phage display library panning was used for conjugation with the AuNP. Phage display is a method to identify novel peptides that binds to the protein targets with high affinity and specificity. This technique has been used for diverse number of applications (Hamzeh-Mivehroud et al. 2013). In particular the identified peptides represent paratopes (antigen binding site of immunoglobulins) and are considered viable alternative to antibodies, hence can be used to develop better diagnostic and anti-infective applications (Ladner et al. 2004; Huang et al. 2012). In recent years, phage display method has been used to identify specific peptides for large number of pathogenic viruses including west nile virus (Bai et al. 2007), hepatitis C virus (Hong et al. 2010), HIV (Welch et al. 2010), influenza virus (Wu et al. 2011). In our experiments, we have used the peptide that was earlier shown to have high selective binding affinity to Newcastle disease virus (NDV) (Ramanujam et al. 2002). The use of such peptides coupled with the AuNP can give higher sensitivity in the visual detection of the virus. The strategy described here involves traditional facile synthesis of AuNP using citrate reduction followed by simple conjugation with cysteinylated peptides taking the advantage of strong gold–sulfur interaction. The prepared peptide–AuNP gave fast and selective visual sensing of virus, and the extent of color changes gave direct correlation with concentration of virus.

Materials and methods

Peptide synthesis

Solid phase methodology with Fmoc chemistry was used to carry out synthesis of peptide (NH_2-TLTTTKLY-Linker-Cys–$CONH_2$). In brief, after 1 h swelling of rink amide MBHA resin (loading capacity 0.42 mol/g of resin, Nova Biochem), 20 % piperidine treatment was done to remove the protecting Fmoc group. The Fmoc–Cys (Trt)–OH as the first amino acid (five equivalent to the loading capacity of the resin) was activated with equivalent amounts of 1-(Bis (dimethylamino) methylene)-1*H*-benzotrizolium hexaflurophosphate (1-) 3 oxide (HBTU) and 1-hydroxybenzotriazol (HOBT) and made to react with the resin in the presence of diisopropyl ethylamine (DIEA). Coupling was allowed for 2 h followed by end capping with acetic anhydride. Loading/coupling efficiency was determined by estimating Fmoc group at each step of synthesis. Using 20 % piperidine (v/v), Fmoc group

from Cys-linked resin was removed. The linker, Fmoc-6-amino hexanoic acid (3 equivalents) activated using HBTU-HOBT, was made to react with Cys on the resin support. Coupling efficiency was measured, and then, Fmoc-Tyr (t-Butyl)-OH was added to the amino end of the linker following similar steps of synthesis. Subsequent deprotection, coupling and end capping were repeated till the completion of synthesis. Peptide was deprotected and cleaved from resin beads using a treatment with Trifluroaceticacid/phenol/thioanisol/1-dodecanethiol/water (82.5:5:5:2.5:5 v/v) mixture for 4 h and precipitated in chilled dry diethyl ether. Precipitated peptides in crude forms were purified by reversed-phase chromatography (RP-HPLC) on a C_{18} - semi-preparative column (7 × 300 mm; 10 μ particle size) using UFLC pump system (Shimadzu, Tokyo, Japan) fitted with photo diode array (PDA) detector. The binary gradient of water/acetonitrile having 0.1 % TFA (v/v) was used for purification of peptide. Peptide was further analyzed for purity on analytical C-18 column (4 × 150 mm; 5 μ particle size).

Synthesis of AuNP

AuNPs were prepared by citrate reduction of $HAuCl_4$. An aqueous solution of $HAuCl_4$ (250 ml, 1 mM) was refluxed for 5–10 min, and a warm aqueous solution of sodium citrate (30 ml, 35 mM) was quickly added. The reflux was continued for another 30 min until a deep red solution was obtained. The solution was passed through 0.45 μ syringe filters to remove any precipitate, and the filtrate was stored at 4 °C until further use.

Conjugation of peptides to AuNP

Peptide (NH_2-TLTTTKLY-Linker-Cys–$CONH_2$) was conjugated to the AuNP by mixing 5 nM of AuNP with different concentrations of peptide to optimize the peptide amount required for activation to avoid excessive peptide-induced precipitation. The mixture (5 ml AuNP + 10 μg peptide) was incubated for 24 h with gentle stirring. The solution was twice washed by centrifugation at 16,000×*g* for 20 min, and the pellet was resuspended in phosphate buffer, pH 7.4. In order to check the absence of nonconjugated peptide, 2 ml of the conjugated solution was centrifuged at 16,000×*g* for 30 min. The supernatant was then evaporated to dryness, re-suspended in mixture of H_2O/acetonitrile (1:1) and analyzed by HPLC to confirm the absence of free peptide. The conjugation peptide on AuNP was analyzed by FTIR on an ATR cell (Nicolet 6700 FTIR, Thermo Fisher) using sample solution drops dried on the FTIR cell surface. Peptide–Cys–AuNPs were first suspended in methanol through sonication to ensure the extraction of representative dispersion volumes. A drop of suspension was then deposited on a carbon-coated copper grid (300 mesh, Electron Microscopy Sciences) and permitted to dry at room temperature. TEM images were taken on a Phillips Biotwin 12 transmission (FEI) electron microscope. Particle size analysis was performed for Peptide–Cys–AuNP conjugates and also after addition of virus solution to Peptide–Cys–AuNP conjugates using a Zetatrac instrument (Microtrac) with built-in liquid sample holder. The concentration of the sample was adjusted for the optimal measurement condition. Three 30 s measurements were averaged for particle size determination.

Virus propagation and titration

In this study, velogenic NDV strain that showed HA titer of 2^8 and further propagated in Hela cells was used. Hela cells were cultivated in Dulbecco's modified eagle's medium (DMEM) (Sigma, USA) supplemented with 10 % fetal bovine serum (Sigma, USA), penicillin 100 U/ml, streptomycin 100 μg/ml, and HEPES buffer (10 mM) (Duchefa Biochemie, The Netherlands). Subconfluent cells were infected with NDV at 0.1 and 0.01 multiplicity of infection (m.o.i.) and harvested at 48 h post-infection (p.i.). The virus stock that contained $10^{7.7}$ $TCID_{50}$ was stored at −80 °C until further use. NDV was also propagated by inoculating in nine-day-old embryonated eggs. After incubation for 5–7 days at 37 °C, eggs are chilled at 4 °C, and allantoic fluid was harvested and tested for HA (Hemagglutination) using chicken RBCs. The allantoic fluid showing HA titer of 2^8 was stored at 4 °C until further use.

Interaction of viral particles with Peptide–Cys–AuNP conjugates

Serial two-fold dilutions of stock virus suspension (HA titer 2^8) were added to each 100 μl of peptide–AuNP conjugate. To check the selectivity of the test, controls were included: plain DMEM + 10 % FCS

and allantoic fluid from uninfected embryo. The visible color changes were observed and compared. The UV–Vis absorption spectra were recorded at wavelengths ranging from 400 to 700 nm for the solutions prepared by taking different concentrations of virus in equal volume (10 µl) of allantoic fluid and added to 90 µl of peptide–Cys–AuNP solutions. Spectra of allantoic fluid alone (10 µl) in water (90 µl) as well as in peptide–Cys–AuNP (90 µl) were also recorded for baseline correction. OD at 520 and 610 nm in different spectra after baseline correction were used to have the ratio metric values (OD_{610}/OD_{520}) in order to draw calibration curves for quantitation.

Results and discussion

Characterization of citrate-stabilized AuNP

Gold nanoparticles were synthesized by reduction of $HAuCl_4$ by sodium citrate following the methods described earlier (Grabar et al. 1995). At high temperature (80–100 °C), citrate helps in reduction and stabilization of gold particles. The color of the solution changed from yellow to dark red wine as the reaction proceeded to completion. The AuNPs were fairly monodispersed with spherical shape, as demonstrated by TEM. The average AuNP size was determined after analyzing 100 particles using ImageJ software, the average core diameters were found to be 20 ± 1.9 nm (Fig. 1A). Concentration of AuNP was measured by volume–density-based method with assumption of 100 % reaction yield. The number of gold atoms per nanoparticles were found to be 250,000. The molar concentration of the nanospheres solution was calculated by dividing the total number of gold atoms based on the initial amount of gold salt added to the reaction solution (1 mM) over the average number of gold atoms per nanosphere (Liu et al. 2007). The AuNP concentration was found to be 4 nM when resuspended in equal volumes of distilled water used during synthesis protocol.

Characterization of Peptide-conjugated AuNP

The synthesized nanoparticles were used for covalent activation with peptides. We used previously identified high-affinity peptide (TLTTKLY) that binds to NDV (Ramanujam et al. 2002). The peptide was identified after three rounds of phage display biopanning using inactivated NDV as target. The surface glycoproteins of NDV (HN and F) which protrude from the viral lipid bilayer membrane acted as binding sites for the selected phages. The phage-derived peptide competitively inhibited the binding of antibodies raised against the intact virion (Ramanujam et al. 2004). This selective inhibition of antibody binding to virus by peptide provides a base for the hypothesis that this peptide can potentially be used for visual viral diagnosis with the help of gold nanoparticles. The projected assay may help to develop affordable visual diagnosis of viral diseases.

AuNPs are popularly functionalized with strong sulfur–gold interface for wide ranging applications including site-specific bio-conjugate labeling and sensing, drug delivery and medical therapy (Häkkinen 2012). In the present assay, we decorated AuNPs with phage display identified anti-NDV peptide with the help of cysteine. It was observed that C-terminal cysteine followed by linker (6-aminohexanoic acid) added to the peptide sequence strongly anchors the peptide to AuNPs. The functionalization of peptides on AuNPs was confirmed by UV–Vis and FTIR spectroscopy. The change in the spectral peaks in the UV–Vis and the peaks due to the presence of amide bond vibrational bands in FTIR spectra of peptide–Cys–AuNP conjugates at different frequency regions (3200–3400 cm^{-1}, N–H stretching; 2900 and 2800 cm^{-1}, CH_2 sym & CH_2 asym stretching; 1697 cm^{-1}, Amide-I C–O stretching; Amide-II C–O bending, 1500 cm^{-1}) indicated the successful conjugation of peptide onto the AuNP surface (Fig. 1B, C).

Colorimetric detection of the virus particles using Peptide–Cys–AuNP conjugates

The scheme of peptide–Cys–AuNP-based detection of virus is shown in Fig. 2. The surface glycoproteins of NDV may bind to the individual AuNP via the conjugated peptide. The interactions between each virus particles with large number of AuNP lead to networking and thus reduce the distance between individual AuNP. In the present visual viral-detection assay, addition of NDV to the peptide–Cys–AuNPs solution resulted in change of original red wine color to purple color, indicative of viral presence in the given solution. Particle analyses were performed

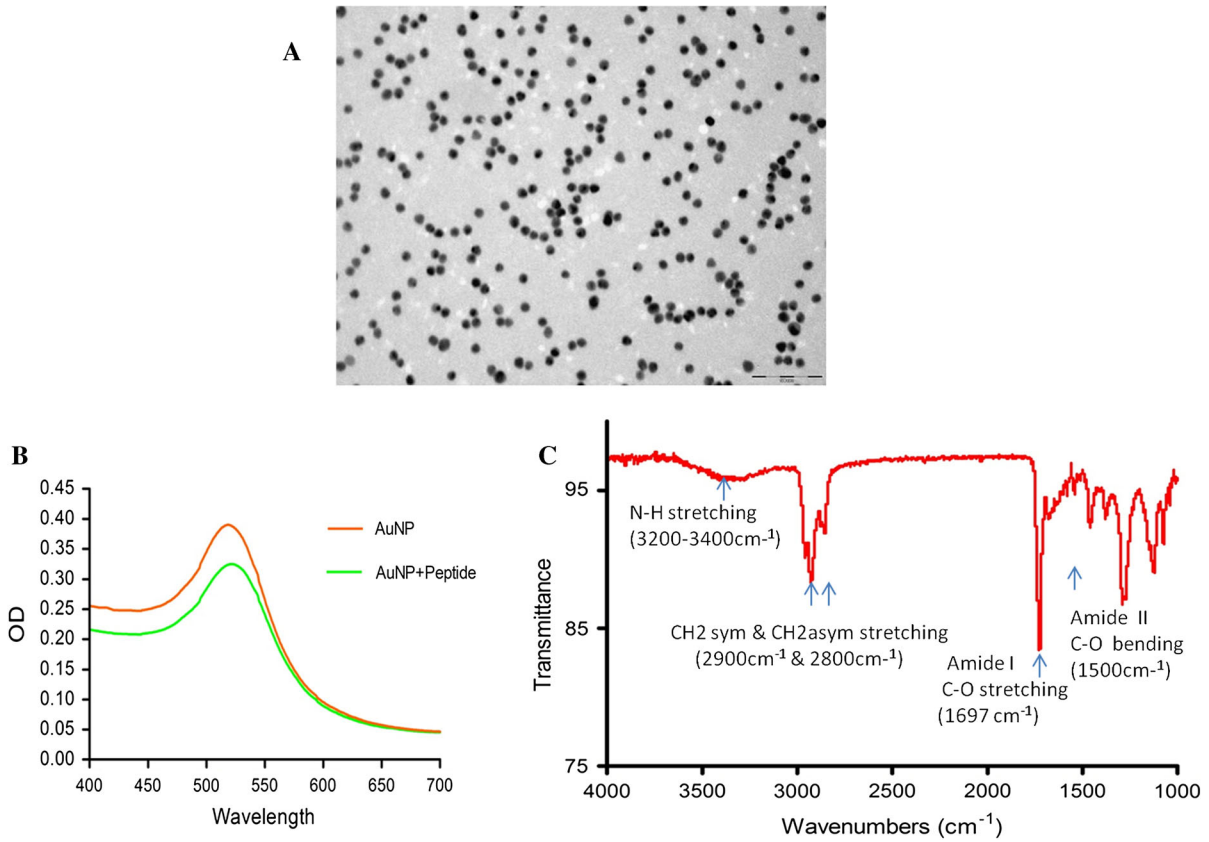

Fig. 1 TEM analysis and activation of citrate-stabilized AuNPs with Peptide-Linker-Cys. The monodispersed particles showing diameter of 20 ± 1.9 nm (**A**); spectral changes before and after conjugation of Cys-peptide on AuNP (**B**); FTIR analysis of peptide–Cys–AuNP showing characteristic peaks (**C**)

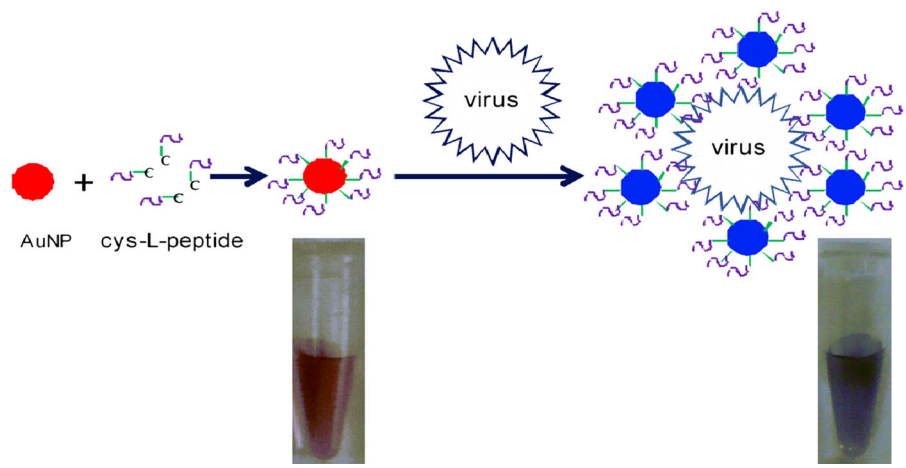

Fig. 2 The scheme of peptide–Cys–AuNP-based detection of virus

before and after the addition of NDV to the AuNP solution using zeta sizer (Microtac instrument). Before the addition of the virus, the AuNP size distribution was represented as a peak at 20 nm. After the addition of NDV to the peptide–Cys–AuNP solution, the size distribution showed a wide range ranging from 20 to

300 nm. This indicated the presence of both individual and aggregated peptide–Cys–AuNP along with the NDV (Fig. 3), and the latter is responsible for the color change.

For spectroscopic detection, absorption spectra (400–700 nm) were recorded every minute after the addition of 10 v % of NDV suspension to 1 nM peptide–Cys–AuNP. Spectra changes immediately after the addition of the virus, indicating the aggregation of AuNPs. Over a period of time, OD_{610} nm increases, while OD_{520} nm decreases. The increased absorbance at 610 nm indicates that AuNP aggregates have formed, thus decreasing the population of single AuNPs as they are converted into AuNP aggregate on the viral particle surface. The spectroscopic measurements were plotted at different time intervals, spectra became stable after 20 min from the beginning of experiment (Fig. 4). Different concentrations of virus in allantoic fluids were added to the peptide–Cys–AuNP in equal volume, and absorption spectra were obtained after reaching the plateau. When change in OD ratios (OD_{610}/OD_{520} was plotted against respective virus concentrations, a linear correlation ($R^2 = 0.995$) was observed. This value of linear coefficient is comparable to the reported values obtained using real-time PCR for detection of NDV (Joshi et al. 2013). The present method avoids tedious method of viral RNA isolation and quantitation (Fig. 5).

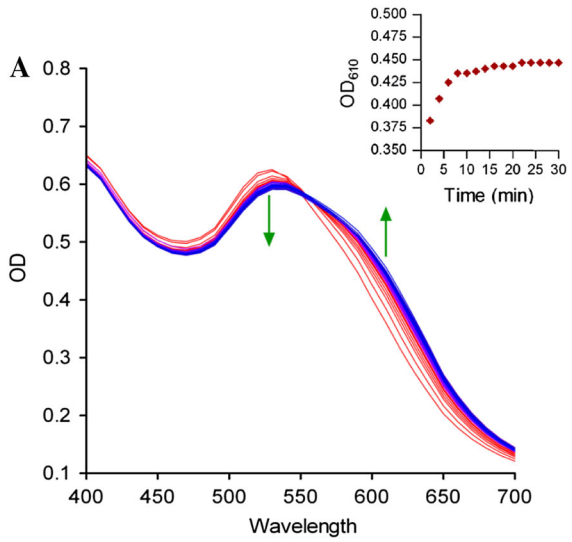

Fig. 4 Interaction of peptide-activated AuNP with the virus. UV–vis absorption spectra measured each at 1 min interval (from 2 to 20 min) after addition of NDV to peptide–Cys–AuNP solution (**A**). The *arrows* indicate decrease in absorbance at 520 nm and increase in absorbance at 610 nm gradually over a period of time (*Inset* change of OD_{610} over a period time after addition of NDV to peptide–Cys–AuNP solution)

Specificity of the virus detection test

To further test the hypothesis that phage-derived peptides interact with NDV, excess of the free peptide solution was incubated with NDV stock to occupy all the binding sites on the surface glycoproteins of NDV. This pretreated virus was then tested with peptide–Cys–AuNP solution, and the absorption spectra were recorded. The observations showed smaller changes in the spectra in pretreated virus samples compared to the nontreated virus (Fig. 6A, B). These results suggest that peptide decorated on AuNP interact in similar manner as that of free peptide with NDV. A stock of NDV propagated in HeLa cells maintained in DMEM with 10 % FBS was utilized as test samples in visual assay. Plain DMEM with 10 % FBS was included as

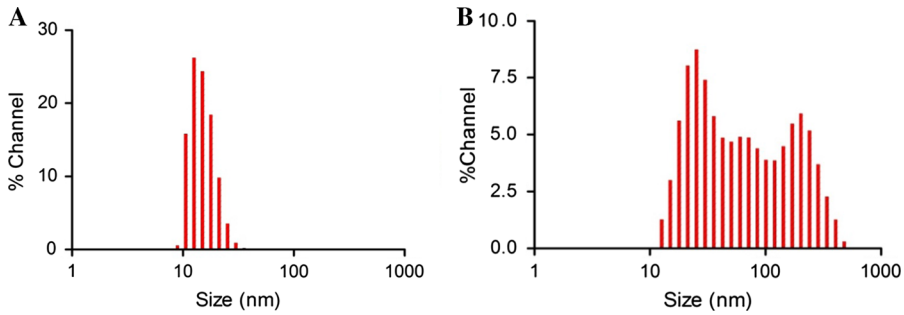

Fig. 3 Particle size distributions of peptide–Cys–AuNPs before (**A**) and after (B) addition of NDV. The increase in the size of particles after addition of virus indicates specific aggregation of peptide-conjugated gold nanoparticles

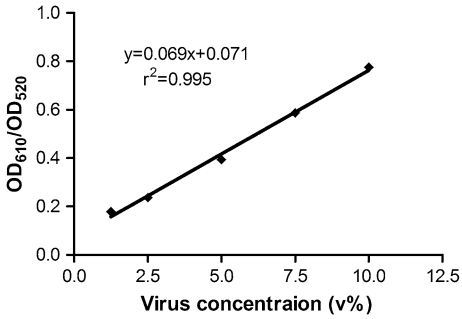

Fig. 5 Calibration curve showing changes in OD ratio (OD_{610}/OD_{520}) after addition of different concentrations of virus (v %) of NDV to peptide–Cys–AuNP solutions with high linear correlation

control in order to determine whether the medium containing salts and other biological components like amino acids and vitamins cause destabilization of colloidal gold. There was no significant change in the visual color of the peptide–Cys–AuNP solutions on addition of blank control samples compared to test samples containing the virus. In case of DMEM which contains pH indicator phenol red that may interfere in spectroscopic quantitation, however, allantoic fluid which is commonly used for NDV field samples did not show any interference. For absolute quantitation, blank base line can be subtracted (Fig. 7). Previously, Lee et al. (2013) employed SA-stabilized AuNP (SA–AuNP) for the colorimetric detection of influenza virus. However, such method of virus detection based on common binding elements may yield false positive results as SA is a part of cellular glycoprotein with which many viruses interact before their entry into the host cells (Neu et al. 2011). When SA–AuNP were used with viruses other than influenza (NDV and Pest des Petits of ruminants virus), similar results were obtained as that of influenza virus (data not shown). In comparison to SA–AuNP-based method, our study involved specific peptide-based viral sensing. This method of using peptide–Cys–AuNP could specifically detect NDV based on visible plasmon changes.

Sensitivity of peptide–Cys–AuNP conjugates in virus detection

In order to determine the sensitivity of peptide–Cys–AuNPs-based NDV detection, the present assay was compared with recommended HA test. NDV has the characteristic property of agglutinating chicken red blood cells. Chicken RBC's (1 %) are routinely used to determine the two fold titer of NDV (Miller and Torchetti 2014). HA test was performed in parallel with the AuNPs-based detection of the virus. The sample of NDV showed HA titer of 2^8 indicating the presence of virus after eight times two fold dilutions. Similarly, when the same sample was used with peptide–Cys–AuNP conjugate, the virus could be detected even after 2^{11} dilutions by clear visible plasmon change (Fig. 8). One HA unit is the highest dilution of the virus which can be detected by the HA test. Accordingly, the results with peptide–Cys–AuNP conjugate indicated that the new method can detect 0.125 HA unit of the virus particles present in the biological samples. The method shows higher sensitivity than the standard HA tests used in NDV detection.

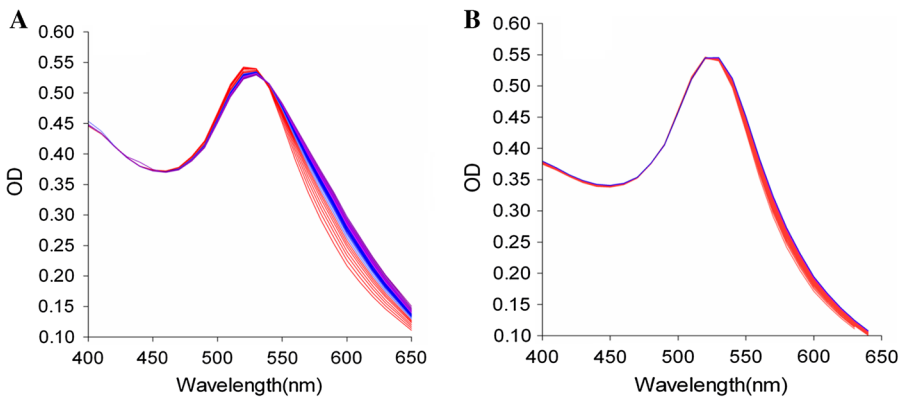

Fig. 6 Effect of pretreatment of NDV with peptide on aggregation of peptide–Cys–AuNP. Peptide–Cys–AuNP incubated with untreated NDV (**A**); peptide–Cys–AuNP incubated with peptide pretreated NDV (**B**)

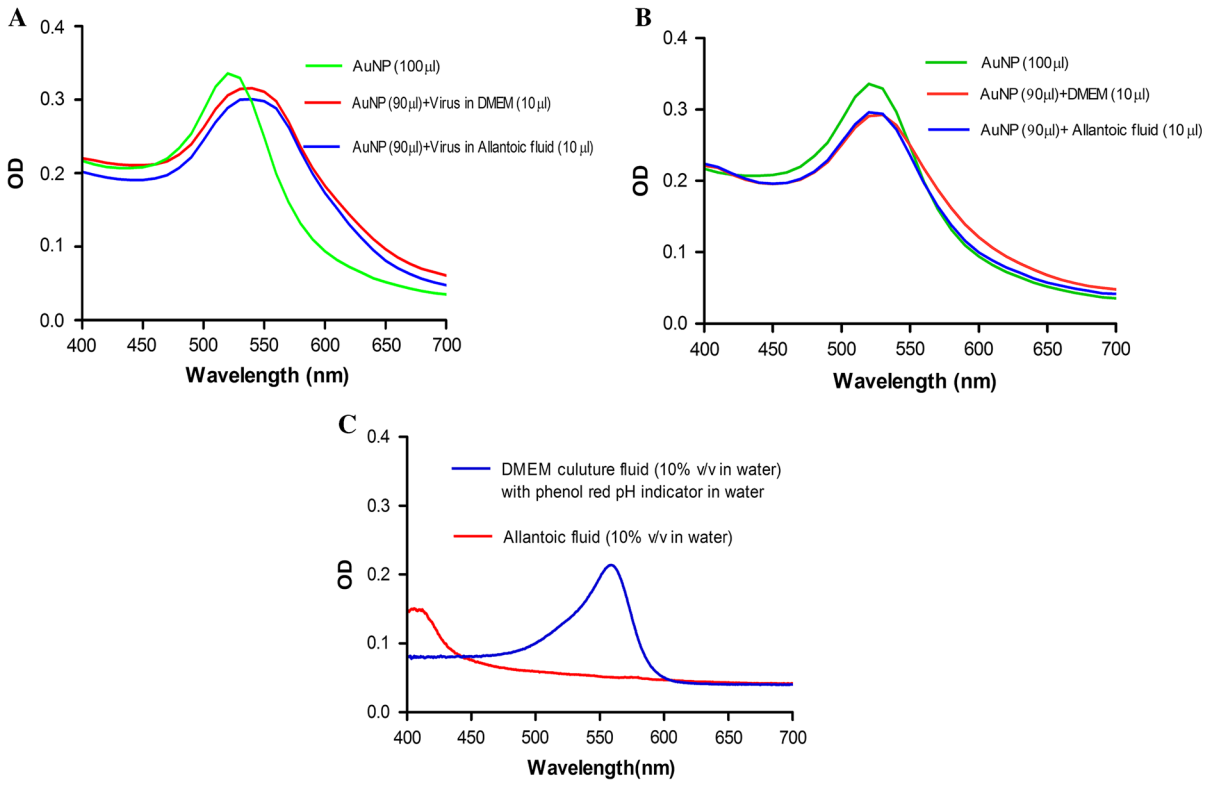

Fig. 7 Absorption spectra of peptide–Cys–AuNP incubated with or without virus (NDV) in different biological samples. The decrease in absorbance at 520 nm and the increase in absorbance at 610 nm were observed when peptide–Cys–AuNP was added to the virus-containing allantoic fluid and DMEM (**A**). There was no significant change observed when allantoic fluid without virus was mixed (**B**), while DMEM culture fluid containing phenol red pH indicator may interfere in virus quantitation experiments (**C**)

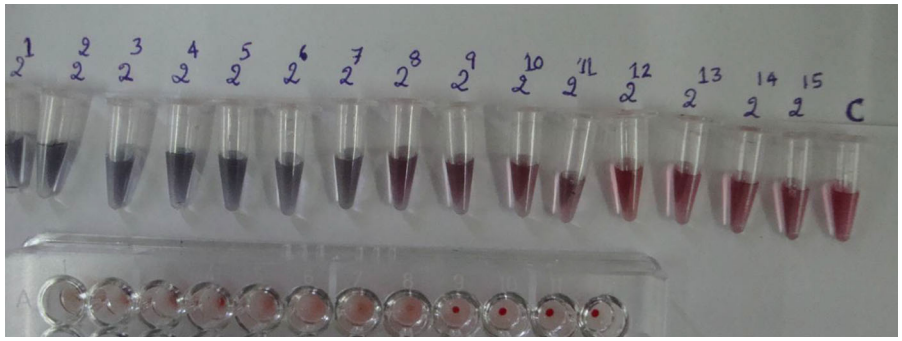

Fig. 8 Comparison of peptide–Cys–AuNP and hemagglutination (HA) test-based visual detection of NDV in allantoic fluid clinical sample. The serial twofold dilutions of virus in the PBS were added to AuNP–Cys–peptide solution (in tubes). Similar dilutions were also added to 1 % chicken RBC (microtitre plate). Visible *color* change to purple is appreciable up to 2^{11} dilution in case of peptide–Cys–AuNP test. However, agglutination of the chicken RBC is visible up to 2^{8} dilution in case of HA test. (Color figure online)

Conclusion

The present study demonstrates the use of virus-specific peptides–Cys–AuNP conjugate for rapid visual diagnostic assay. Cysteinylated peptide ligand to virus was used for functionalization of AuNPs. The results of the experiments indicated that peptide–Cys–AuNP can specifically detect the virus both in culture suspensions and in biological samples like infected allantoic fluid. Further peptide–Cys–AuNP-based test is more sensitive compared to the standard HA test for NDV. The limit of detection of the test was 0.125 HA units of the virus. The general scheme envisaged in the present study may be useful in detecting animal viruses based on specific peptide conjugated to AuNPs with improved sensitivity. The method does not require isolation of viral RNA, as quantification may be made by direct measurement of color changes with virus concentrations.

Acknowledgment The authors are thankful to the Director, the Indian Veterinary Research Institute, Bareilly-243122 (UP) India and the Department of Biotechnology (GOI) for providing research Grant and facilities.

References

Bai F, Town T, Pradhan D, Cox J, Ashish Ledizet M, Anderson JF, Flavell RA, Krueger JK, Koski RA, Fikrig E (2007) Antiviral peptides targeting the west nile virus envelope protein. J Virol 81(4):2047–2055

Belák S (2007) Molecular diagnosis of viral diseases, present trends and future aspects a view from the OIE collaborating centre for the application of polymerase chain reaction methods for diagnosis of viral diseases in veterinary medicine. Vaccine 25:5444–5452

Cobo F (2012) Application of molecular diagnostic techniques for viral testing. Open Virol J 6:104–114

Darbha GK, Singh AK, Rai US, Yu E, Yu H, Chandra Ray P (2008) Selective detection of mercury (II) ion using non-linear optical properties of gold nanoparticles. J Am Chem Soc 130(25):8038–8043

Grabar KC, Freeman RG, Hommer MB, Natan MJ (1995) Preparation and characterization of Au colloid monolayers. Anal Chem 67:735–743

Häkkinen H (2012) The gold-sulfur interface at the nanoscale. Nat Chem 4(6):443–455

Hamzeh-Mivehroud M, Alizadeh AA, Morris MB, Church WB, Dastmalchi S (2013) Phage display as a technology delivering on the promise of peptide drug discovery. Drug Discov Today 18(23–24):1144–1157

Hong HW, Lee SW, Myung H (2010) Selection of peptides binding to HCV e2 and inhibiting viral infectivity. J Microbiol Biotechnol 20(12):1769–1771

Huang JX, Bishop-Hurley SL, Cooper MA (2012) Development of anti-infectives using phage display: biological agents against bacteria, viruses, and parasites. Antimicrob Agents Chemother 56(9):4569–4582

Jin R, CaoY Mirkin CA, Kelly KL, Schatz GC, Zheng JG (2001) Photoinduced conversion of silver nanospheres to nanoprisms. Science 294(5548):1901–1903

Joshi VG, Chindera K, Singh AK, Sahoo AP, Dighe VD, Thakuria D, Kumar S (2013) Rapid label-free visual assay for the detection and quantification of viral RNA using peptide nucleic acid (PNA) and gold nanoparticles (AuNPs). Anal Chim Acta 795:1–7

Ladner RC, Sato AK, Gorzelany J, de Souza M (2004) Phage display-derived peptides as therapeutic alternatives to antibodies. Drug Discov Today 9(12):525–529

Lee C, Gaston MA, Weiss AA, Zhang P (2013) Colorimetric viral detection based on sialic acid stabilized gold nanoparticles. Biosens Bioelectron 42:236–241

Lesniewski A, Los M, Jonsson-Niedzioka M, Krajewska A, Szot K, Los JM, Niedziolka-Jonsson J (2014) Antibody modified gold nanoparticles for fast and selective, colorimetric T7 bacteriophage detection. Bioconjugate Chem 25(4):644–648

Liu X, Atwater M, Wang J, Huo Q (2007) Extinction coefficient of gold nanoparticles with different sizes and different capping ligands. Coll Surf B Biointerfaces 58(1):3–7

Matrosovich M, Herrler G, Klenk HD (2013) Sialic acid receptors of viruses. Top Curr Chem, Springer, Berlin. doi: 10.1007/128_2013_466

Medley CD, Smith JE, Tang Z, Wu Y, Bamrungsap S, Tan W (2008) Gold nanoparticle-based colorimetric assay for the direct detection of cancerous cells. Anal Chem 80(4):1067–1072

Miller PJ, Torchetti MK (2014) Newcastle disease virus detection and differentiation from avian influenza. Methods Mol Biol 1161:235–239

Neu U, Bauer J, Stehle T (2011) Viruses and sialic acids: rules of engagement. Curr Opin Struct Biol 21(5):610–618

O'Connor L, Glynn B (2010) Recent advances in the development of nucleic acid diagnostics. Expert Rev Med Devices 7(4):529–539

Ramanujam P, Tan WS, Nathan S, Yusoff K (2002) Novel peptides that inhibit the propagation of Newcastle disease virus. Arch Virol 147(5):981–993

Ramanujam P, Tan WS, Nathan S, Yusoff K (2004) Pathotyping of Newcastle disease virus with a filamentous bacteriophage. Biotechniques 36(2):296–300

Rita MC, Pedro BV (2014) Anti-cancer precision theranostics: a focus on multifunctional gold nanoparticles. Expert Rev Mol Diagn 14(8):1041–1052

Stehle T, Khan ZM (2014) Rules and exceptions: sialic acid variants and their role in determining viral tropism. J Virol 88(14):7696–7699

Welch BD, Francis JN, Redman JS, Paul S, Weinstock MT, Reeves JD, Kay MS (2010) Design of a potent D-peptide HIV-1 entry inhibitor with a strong barrier to resistance. J Virol 84(21):11235–11244

West JL, Halas NJ (2000) Applications of nanotechnology to biotechnology. Curr Opin Biotechnol 11:215–217

Wu D, Li G, Qin C, Ren X (2011) Phage displayed peptides to avian H5N1 virus distinguished the virus from other viruses. PLoS One 6(8):e23058